A FINITE ELEMENT METHOD BASED ON THE ENHANCED FIRST ORDER SHEAR DEFORMATION THEORY FOR COMPOSITE AND SANDWICH STRUCTURES

Jinho Oh*, Maenghyo Cho , Jun-Sik Kim*****

*** Seoul National University, San 56-1, Shillim-Dong, Kwanak-Gu, Seoul 151-744, Korea**
**** Seoul National University, San 56-1, Shillim-Dong, Kwanak-Gu, Seoul 151-744, Korea**
*****The Pennsylvania State University, University Park, PA 16802, U.S.A.**

Keywords: *First Order Shear Deformation Theory; Enhanced First Order Shear Deformation Theory; Laminated Composite; Higher Order Zig-zag Theory; Finite Element Formulation;*

Abstract

The finite element formulation based on enhanced first order shear deformation theory is developed to accurately and efficiently predict the behavior of laminated composite and sandwich structures. The enhanced first order shear deformation theory is systematically derived by minimizing the least-squared strain energy error between the first order theory and the higher order theory. This makes it possible implement finite element method based on the C_0 shape function by transforming the strain energy of a higher order zigzag theory to that of a first order zigzag theory. Thus, the proposed finite element formulation will be widely used in various application fields. Through numerical examples, the accuracy and robustness of the present method are demonstrated.

1 Introduction

Until now, various composite plate/shell models have been developed to analyze the composite and sandwich structures efficiently and accurately. Among many proposed models, a higher order zig-zag theory[1,2] is an efficient method to predict accurately deformations and stresss through the thickness of laminated structures. Higher-order zigzag theory(HOZT) satisfies transverse stress conditions as well as displacement continuity conditions through the thickness of the laminates. HOZT was extended to weakly coupled and fully coupled thermo-electric-mechanical behavior of smart composite plates[3,4].

HOZT requires only degrees of freedom defined at the reference plane and not requires layer-dependent degrees of freedom. Thus this theory has computational advantage when thick multilayered composite structures are required to be analyzed. However, this higher order zig-zag theory requires C_1 shape functions(slope continuity condition along the boundary of the element) in the finite element implementation. These shape functions are not conventional in commercial finite element software. This unconventional shape function routine makes harder assemble this special zigzag plate element with other standard isoparametric elements. To overcome this drawback, an enhanced first order shear deformation theory(EFSDT)[5] is developed. It requires only C_0 shape functions in finite element formulation.

In the present study, the developed finite element based on EFSDT is evaluated through several numerical examples. The accuracy and robustness of the present FE method based on EFSDT are demonstrated.

2 Formulation of Enhanced First Order Shear Deformation Theory

2.1 Displacement Formulation

The general form of displacement field of the interior solution to describe the behavior of laminated plates can be expressed by

$$u_\alpha(x_i) = u^o_\alpha(x_\beta) - u^o_{3,\alpha}(x_\beta)\, x_3 + W_\alpha(x_i) \qquad (1)$$

$$u_3(x_i) = u_3^o(x_\beta) + W_3(x_i) \tag{2}$$

in which, $W_\alpha(x_i)$ and $W_3(x_i)$ represent warping functions. The in-plane displacement fields of higher order zig-zag theory are constructed by super-imposing linear zig-zag field to the smooth globally cubic varying field through the thickness. The final displacement fields are expressed in terms of the reference primary degrees of freedom by applying interface continuity conditions as well as bounding surface conditions of transverse shear stresses. The final displacement field is written as follows:

$$\begin{aligned} u_\alpha &= u_\alpha^o - u_{3,\alpha}^o x_3 + x_3^3 \frac{1}{3}\phi_\alpha - \frac{h^2}{4} x_3 \phi_\alpha \\ &- \frac{x_3}{2}\sum_{k=1}^{N-1} a_{\alpha\gamma}^{(k)} \phi_\gamma - x_3^2 \frac{1}{2h}\sum_{k=1}^{N-1} a_{\alpha\gamma}^{(k)} \phi_\gamma \\ &+ \sum_{k=1}^{N-1} a_{\alpha\gamma}^{(k)} \phi_\gamma (x_3 - x_3^{(k)}) H(x_3 - x_3^{(k)}) \end{aligned} \tag{3}$$

The warping functions are obtained by minimizing the errors between the averaged strain and displacement of the first order theory and the strains and displacement of higher order theory in the least-square sense. This can be expressed as the following compact form.

$$\begin{aligned} u_\alpha(x_i) &= u_\alpha^o(x_\alpha) - u_{3,\alpha}^o(x_\alpha) x_3 + \Phi_{\alpha\gamma}^{(0)}(x_3)\phi_\gamma(x_\alpha) \\ u_3(x_i) &= u_3^o(x_\alpha) \end{aligned} \tag{4}$$

The strains associated with the small displacement theory of elasticity are given by

$$\varepsilon_{\alpha\beta}(x_i) = \varepsilon_{\alpha\beta}^{(o)}(x_\alpha) + x_3 \varepsilon_{\alpha\beta}^{(1)}(x_\alpha) + \varepsilon_{\alpha\beta}^{(w)}(x_i), \tag{5}$$

and transverse shear strains are expressed as

$$\begin{aligned} \gamma_{3\alpha}(x_i) &= u_{\alpha,3} + u_{3,\alpha} \\ &= \Phi_{\alpha\gamma,3}^{(0)}(x_3)\phi_\gamma(x_\beta) + W_{3,\alpha} \end{aligned} \tag{6}$$

The warping function W_3 presented Eq. (6) is very small compared to the effective transverse shear strains in the variational-asymptotic sense[4]. Then, transverse shear strains are expressed in terms of the effective shear strains $\phi_\alpha^{(k)}$ only.

$$\gamma_{3\alpha} \cong \Phi_{\alpha\gamma,3}^{(0)}(x_3)\phi_\gamma(x_\beta) \tag{7}$$

2.2 Relationships between Variables of Higher Order Theory and Those of First Order Theory

The warping functions are obtained by minimizing the errors between the averaged strain and displacement of the first order theory and the strains and displacement of higher order theory in the least-square sense.

$$\begin{aligned} &\min_{\bar{\varepsilon}_{\alpha\beta}^o} \langle \| \varepsilon_{\alpha\beta} - \bar{\varepsilon}_{\alpha\beta} \|_2 \rangle = 0 \rightarrow \\ &\bar{\varepsilon}_{\alpha\beta}^o = \varepsilon_{\alpha\beta}^{(0)} + \frac{1}{h}\left\langle x_3^2 \right\rangle \varepsilon_{\alpha\beta}^{(2)} + \frac{1}{h}\langle \varepsilon_{\alpha\beta}^{(w)} \rangle \end{aligned} \tag{8}$$

$$\begin{aligned} &\min_{\kappa_{\alpha\beta}} \langle \| \varepsilon_{\alpha\beta} - \bar{\varepsilon}_{\alpha\beta} \|_2 \rangle = 0 \rightarrow \\ &\kappa_{\alpha\beta} = \varepsilon_{\alpha\beta}^{(1)} + \frac{12}{h^3}\left\langle x_3^4 \right\rangle \varepsilon_{\alpha\beta}^{(3)} + \frac{12}{h^3}\langle x_3 \varepsilon_{\alpha\beta}^{(w)} \rangle \end{aligned} \tag{9}$$

$$\begin{aligned} &\min_{\bar{u}_\alpha^o} \langle \| u_\alpha - \bar{u}_\alpha \|_2 \rangle = 0 \rightarrow \\ &\bar{u}_\alpha^o = u_\alpha^o - \frac{1}{h}\left\langle x_3^2 \right\rangle r_{1,\alpha} + \frac{1}{h}\langle W_\alpha \rangle \end{aligned} \tag{10}$$

$$\begin{aligned} &\min_{\theta_\alpha} \langle \| u_\alpha - \bar{u}_\alpha \|_2 \rangle = 0 \rightarrow \\ &\theta_\alpha = -u_{3,\alpha} - \frac{12}{h^3}\left\langle x_3^4 \right\rangle r_{2,\alpha} + \frac{12}{h^3}\langle x_3 W_\alpha \rangle \end{aligned} \tag{11}$$

$$\begin{aligned} &\min_{\bar{u}_3^o} \langle \| u_3 - \bar{u}_3 \|_2 \rangle = 0 \rightarrow \\ &\bar{u}_3^o = u_3^o + \frac{1}{h}\langle W_3 \rangle \end{aligned} \tag{12}$$

The above equations (Eqs.8-12) minimize the errors of the in-plane stresses in the least-square sense. These equations can be also derived by transforming the three-dimensional strain energy of Eq.(13) into Reissner-Mindlin-like plate theory.

The strain energy expression is given by

$$\begin{aligned} 2U &= \varepsilon_0^T A \varepsilon_0 + 2\varepsilon_0^T B K_0 + K_0^T D K_0 + \phi^T G \phi \\ &+ 2\varepsilon_0^T E K_h + 2K_0^T F K_h + K_h^T H K_h \end{aligned} \tag{13}$$

To utilize the variables of Reissner-Mindlin's plate model, the strain energy should be expressed by the form of Eq. (13). The Eq. (14) is obtained by substituting Eqs. (8)-(12) into Eq. (13)

$$
\begin{aligned}
2U = &\left(\bar{\varepsilon}_0 - \tilde{C}\kappa_h\right)^T A\left(\bar{\varepsilon}_0 - \tilde{C}\kappa_h\right) \\
&+ 2\left(\bar{\varepsilon}_0 - \tilde{C}\kappa_h\right)^T B\left(\bar{\kappa}_o - \tilde{\Gamma}\kappa_h\right) \\
&+ \left(\bar{\kappa}_o - \tilde{\Gamma}\kappa_h\right)^T D\left(\bar{\kappa}_o - \tilde{\Gamma}\kappa_h\right) \\
&+ \bar{\gamma}^T\left(\hat{\Gamma}^T G\hat{\Gamma}\right)\bar{\gamma} + 2\left(\bar{\varepsilon}_0 - \tilde{C}\kappa_h\right)^T E\kappa_h \\
&+ 2\left(\bar{\kappa}_o - \tilde{\Gamma}\kappa_h\right)^T F\kappa_h + \kappa_h^T H\kappa_h
\end{aligned} \tag{14}
$$

After rearranging the energy expression of Eq. (14), the classified two kinds of energies are obtained as follows.

$$
2U = \bar{\varepsilon}_0^T A\bar{\varepsilon}_0 + 2\bar{\varepsilon}_0^T B\bar{\kappa}_0 + \bar{\kappa}_0^T D\bar{\kappa}_0 + \bar{\gamma}^T\hat{G}\bar{\gamma} + 2\tilde{U} \tag{15}
$$

where the remaining energy is expressed as,

$$
\begin{aligned}
2\tilde{U} = &\, 2\bar{\varepsilon}_0^T\left(-A\tilde{C} - B\tilde{\Gamma} + E\right)\kappa_h \\
&+ 2\bar{\kappa}_0^T\left(-B^T\tilde{C} - D\tilde{\Gamma} + F\right)\kappa_h \\
&+ \kappa_h^T\left(\tilde{C}^T A\tilde{C} + 2\tilde{C}^T B\tilde{\Gamma} - 2\tilde{C}^T E + \tilde{\Gamma}^T D\tilde{\Gamma} - 2\tilde{\Gamma}^T F + H\right)\kappa_h
\end{aligned} \tag{16}
$$

The strain energy can be expressed in terms of the conventional Reissner-Mindlin's variables by minimizing energy difference between HOZT and EFSDT. The effective transverse shear stiffness obtained from correlation equation is defined as follows.

$$
\hat{G} = \hat{\Gamma}^T G\hat{\Gamma}, \qquad \hat{e}_o^j = \Gamma^{-T} e_o^j \tag{17}
$$

2.3 Recovery Processing

In this section, the recovery process after completing finite element solution process based on the enhanced first-order shear deformation theory (EFSDT) is described. The modified version of an efficient higher-order theory[1,2] is utilized for the analysis of laminated composite and sandwich structures. Three-dimensional strain energy per unit area is expressed in terms of the averaged strains. Explicit relations between three-dimensional and averaged displacement fields are derived via the least-square approximation of in-plane displacements, strains and stresses that are presented in previous section.

Finally, in the post-processing phase, the final displacement fields are recovered by the following relationship.

$$
\begin{aligned}
u_\alpha &= \bar{u}_\alpha^0 - \bar{u}_{3,\alpha}^0 x_3 - C_{\alpha\gamma}^{(0)}\phi_\gamma + \Phi_{\alpha\gamma}\left(x_3\right)\tilde{\Gamma}_{\gamma\mu}\bar{\gamma}_{3\mu}, \\
u_3 &= \bar{u}_3^0
\end{aligned} \tag{18}
$$

The strain fields can also be recovered by

$$
\begin{aligned}
\varepsilon_{\alpha\beta} &= \bar{\varepsilon}_{\alpha\beta}^o + \frac{1}{h}\left\langle x_3^2\right\rangle\bar{r}_{1,\alpha\beta} - \frac{1}{h}\left\langle\tilde{\Phi}_{\alpha\gamma}^e\hat{\Gamma}\bar{\gamma}_{,\beta}\right\rangle \\
\varepsilon_{3\alpha} &= \tilde{\Phi}_{\alpha\beta}^s\hat{\Gamma}\bar{\gamma}
\end{aligned} \tag{19}
$$

in which, the averaged nodal variables are obtained from results of commercial FE software ANSYS. The derivatives of nodal variables are calculated by using differential quadrature[7]. The differential quadrature method is very simple and efficient numerical approach to solve partial differential equations. The partial derivatives of a function with respect to a variable at any discrete point are approximated into weighted linear sums of the function values at all the discrete points in overall chosen domain.

$$
f_x^{(n)}(x_i, y_j) = \sum_{k=1}^{N_x} C_{ik}^{(n)} f(x_k, y_j) \quad n = 1, 2, ..., (N_x - 1) \tag{20}
$$

$$
f_y^{(m)}(x_i, y_j) = \sum_{k=1}^{N_y} \bar{C}_{jk}^{(m)} f(x_i, y_k) \quad m = 1, 2, ..., (N_y - 1) \tag{21}
$$

$$
\begin{aligned}
&f_{xy}^{(n+m)}(x_i, y_j) = \sum_{k=1}^{N_x} C_{ik}^{(n)} \sum_{l=1}^{N_y} \bar{C}_{jl}^{(m)} f(x_k, y_l) \\
&\quad i = 1, 2, ..., N_x \;\; and \;\; j = 1, 2, ..., N_y
\end{aligned} \tag{22}
$$

where N_x is the number of grid points in the *x*-direction and N_y in the *y*-direction. Numbers *n* and *m* represent the order of the derivatives with respect to *x* and *y* direction. $C_{ij}^{(n)}$ and $\bar{C}_{ij}^{(m)}$ are weighting coefficients.

$$
\begin{aligned}
&C_{ij}^{(n)} = n\left(C_{ii}^{(n-1)}C_{ij}^{(1)} - \frac{C_{ij}^{(n-1)}}{x_i - x_j}\right) \\
&for \quad i, j = 1, 2, \ldots, N_x \\
&j \neq i \quad and \quad n = 2, 3, \ldots, N_y - 1
\end{aligned} \tag{23}
$$

$$
\begin{aligned}
&\bar{C}_{ij}^{(m)} = m\left(\bar{C}_{ii}^{(m-1)}\bar{C}_{ij}^{(1)} - \frac{\bar{C}_{ij}^{(m-1)}}{y_i - y_j}\right) \\
&for \quad i, j = 1, 2, \ldots, N_y \\
&j \neq i \quad and \quad m = 2, 3, \ldots, N_y - 1
\end{aligned} \tag{24}
$$

$$C_{ii}^{(n)} = -\sum_{j=1,\ j\neq i}^{N_x} C_{ij}^{(n)} \quad for \quad i,j = 1,2,\ldots,N_x \quad and \quad n = 1,2,3,\ldots,N_x - 1 \tag{25}$$

$$\bar{C}_{ii}^{(m)} = -\sum_{j=1,\ j\neq i}^{N_y} C_{ij}^{(m)} \quad for \quad i,j = 1,2,\ldots,N_y \quad and \quad m = 1,2,3,\ldots,N_y - 1 \tag{26}$$

Where

$$C_{ij}^{(1)} = \frac{M^{(1)}(x_i)}{(x_i - x_j)M^{(1)}(x_j)} \qquad i,j = 1,2,\ldots,N_x \ \ but \ \ j \neq i$$

$$\bar{C}_{ij}^{(1)} = \frac{P^{(1)}(y_i)}{(y_i - y_j)P^{(1)}(y_j)} \qquad i,j = 1,2,\ldots,N_y \ \ but \ \ j \neq i$$

$$M^{(1)}(x_i) = \prod_{j=1,\ j\neq i}^{N_x}(x_i - x_j),$$

$$P^{(1)}(y_i) = \prod_{j=1,\ j\neq i}^{N_y}(y_i - y_j)$$

The summary of the proposed finite element procedure is given as follows: Firstly, the effective stiffness matrixes are obtained by considering the warping function dependent on the layer material and geometric properties. Secondly, after substituting the stiffness by the effective stiffness, the modeling and analysis of composite and sandwich structures is performed in ANSYS software. Lastly, the recovery procedures to get the detailed deformation and transverse stresses are carried out in the in-house code.

2.4 Numerical Results

The finite element formulation based on the EFSDT is performed by using ANSYS software. This software is applicable since it has 'SHELL99' element based on the C_0 shape functions. Through several numerical examples, the accuracy and robustness of the present finite element method based on EFSDT are demonstrated.

The exact solutions for bending problem of cross-ply laminated plates proposed by Pagano[8] are used as the benchmark solution for the present theory.

The ply material properties in cross-ply laminated plates are given as

$$E_L / E_T = 25, G_{LT} / E_T = 0.5, \quad G_{TT} / E_T = 0.2, \nu_{LT} = \nu_{TT} = 0.25 \tag{27}$$

where L denotes a fiber direction and T denotes a perpendicular direction to the fiber. For a sandwich plate shown in Fig. 6, the material properties of a face sheet are given by Eq. (28), and the core material properties[9] are taken as

$$E_x = 1.0\times10^8\,\text{Pa}\ \left(=0.145\times10^5\,\text{psi}\right),\ E_2 = E_3$$
$$G_{13} = 0.4\times10^8\,\text{Pa}\ \left(=0.58\times10^4\,\text{psi}\right),$$
$$G_{23} = G_{12} = G_{13},\ \nu_{12} = 0.25 \tag{28}$$

The length-to-thickness ratios, $S = 4$ and $S = 10$ value, are evaluated. The in-plane and transverse stresses are plotted. They are important in strength design of composite structures.

Three cases are considered in the present examples.

Case I: Eight-layer regular quadrilateral plate [90/0/90/0/0/90/0/90] with simply-supported boundary condition along the edge under distributed uniform loading.

The comparison of center deflection is shown in Table 1. It is confirmed that the results of the finite element based on the enhanced first order shear deformation theory (EFSDT) agrees very well with those of higher order zigzag theory(HOZT). The displacement of rectangular composite plate is shown in Fig. 1. In-plane stress σ_{xx} through the thickness is depicted in Fig. 2. The comparison of the transverse shear stress is shown in Fig. 3. The discrepancy between EFSDT and FSDT is observed because EFSDT considered the warping function of higher order zig-zag theory. The results of the EFSDT are well correlated with that of higher order zig-zag theory.

Case II: Eight-layer stiffened laminated composite panel [0/90/45/-45/-45/45/90/0] with clamped boundary condition at one side edge under uniform loading.

The dimensions of the stiffened composite panel model are such that length a=20 m, width b=14 m and thickness h=1. Fig. 4 shows the out-of-plane displacement contour of stiffened composite panel. Fig. 5 indicates that the conventional Mindlin/ Reissner type shell element considering shear correction factor of ANSYS software cannot predict accurately transverse shear stress through the thickness very well in angle ply case. But, EFSDT and its post-process recovery routine are capable to predict the detailed deformation and stress behavior through the thickness accurately.

Case III: A simply supported $[0^o/\text{Core}/0^o]$ sandwich plate with the thickness of each face sheet equal to h/10 is considered to investigate a significant shear deformation effect. The uniform loading is distributed over the whole x-y plane. The results from EFSDT clearly indicate in-plane and transverse stresses. However, results of FSDT can not predict in detail. It is obvious that FSDT is not adequate in predicting the local response of sandwich plates.

For more accurate prediction of the transverse shear stresses of sandwich plate, the effect of transverse normal deformation should be considered. The reason is that the core material of a sandwich plate is very flexible compared to the face sheet. The proposed method doesn't consider the transverse normal effect. However, the proposed least-square method has a merit in that it always gives better results than the FSDT while it retains the same computational cost.

3 Conclusions

A finite element method based on the EFSDT has been developed to predict the behaviors of composite/sandwich plates in an efficient and accurate manner. To approximate the through-the-thickness warping functions, the higher order zig-zag displacement fields are modified. The key feature of the present paper is that the applicability of EFSDT on the commercial software is shown by using relationship between energies of the EHOPT and the averaged FSDT derived in the averaged least square sense. The accuracy and robustness of the present method have been demonstrated by comparing the present solutions with higher order zigzag theory solution and the three-dimensional elasticity solutions.for simply-supported laminated and sandwich plates. The FSDT severely underestimated the displacements and stresses, while an EFSDT has shown good agreements with exact elasticity solutions. Thus, the proposed finite element using ANSYS software is a proper method to accurately and efficiently analyze the laminated composite and sandwich structures without significant modifications from FSDT.

References

[1] Cho, M. and Parmerter, R. R., "An efficient higher-order plate theory for laminated composites," *Comp. Struc.* Vol. 20, pp 113-123, 1992.

[2] Cho, M. and Parmerter, R. R., "Efficient higher-order composite plate theory for general lamination configurations," *AIAA Journal,*. Vol. 31, pp 1299-1306, 1993.

[3] Cho, M. and Oh, J., "Higher order zig-zag plate theory under thermo-electric-mechanical loads combined," *Composites B*, Vol. 34, No. 1, pp. 67-82, 2002.

[4] Cho, M. and Oh, J., "Higher order zig-zag theory for fully coupled thermo-electric-mechanical smart composite plates," *Int J Solds Struc*, Vol. 41, pp.1331-1356, 2004

[5] Kim, J. S. and Cho, M., "Enhanced modeling of laminated and sandwich plates via strain energy transformation," *Compos Sci & Tech*, Vol. 66, No. 11-12, pp 1575-1587, 2006.

[6] Yu, W., Hodges, D.H., and Bolovoi, V.V., "Asymptotic construction of Reissner-like composite plate theory with accurate strain recovery," Vol. 31, *Int J Solds Struc*, Vol. 39, pp. 5185-203, 2002.

[7] Liew, K. M., "Differential Quadrature Method for Mindlin Plates on Winkler Foundations," *Int. J. Mech. Sci*, Vol. 38, No. 4, pp. 405-421, 1996.

[8] Pagano, N. J., "Exact solutions for rectangular bidirectional composites and sandwich plates," *Journal of Composite Materials*, Vol. 3, pp. 398-441, 1970.

[9] Rao K.M and Meyer-Piening H.R., "Analysis of sandwich plates using a hybrid-stress finite element," *AIAA Journal*, Vol. 29, pp. 1498-1506, 1991.

Table1. Center deflection $\bar{u}_3$ under distributed loading

S=*a*/*h*	HOZT_FEM	EFSDT	ANSYS	FSDT
4	2.78	2.77	2.32	2.054
10	1.025	1.025	0.96	0.915

$\bar{u}_3 = u_3 100 E_2 h^3/(Pa^4)$

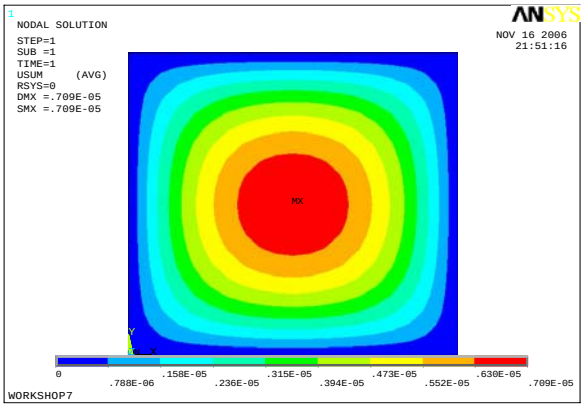

Fig. 1. Displacement contour of rectangular composite plate under uniform loading (S=4)

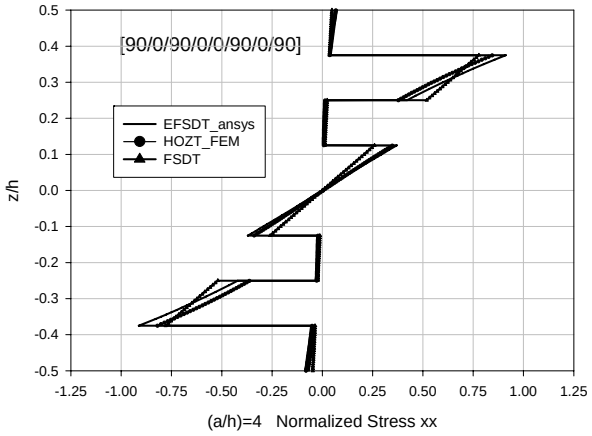

Fig. 2(a). In-plane stress xx $\overline{\sigma}_x = \sigma_x / q_0 S^2$ under uniform loading

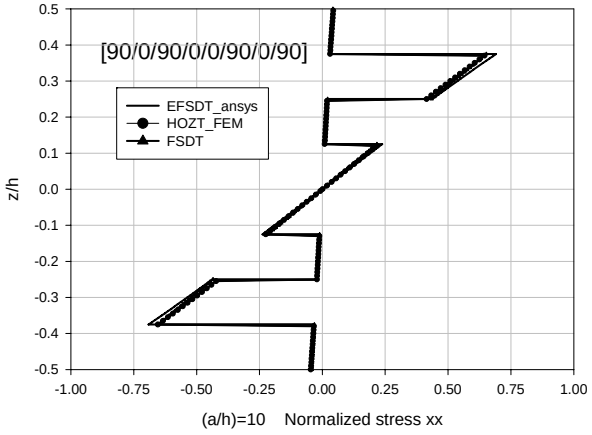

Fig. 2(b). In-plane stress xx $\overline{\sigma}_x = \sigma_x / q_0 S^2$ under uniform loading

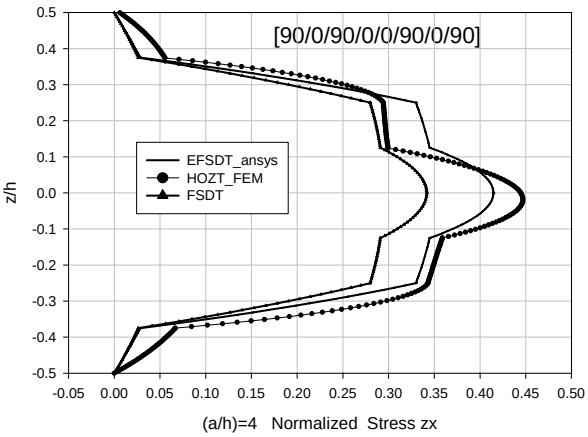

Fig. 3(a). In-plane stress xx $\overline{\sigma}_x = \sigma_x / q_0 S^2$ under uniform loading

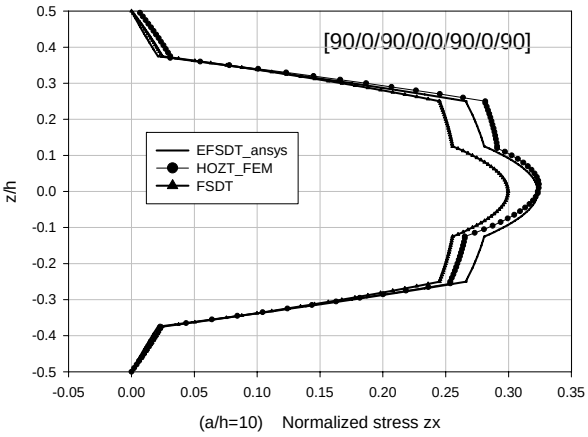

Fig. 3(b). Transverse shear stress zx $\overline{\sigma}_{zx} = \sigma_{zx} / q_0 S$ under uniform loading

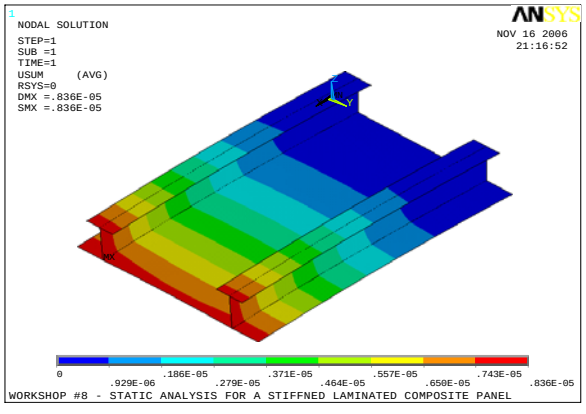

Fig. 4. Displacement contour of stiffened laminated composite panel

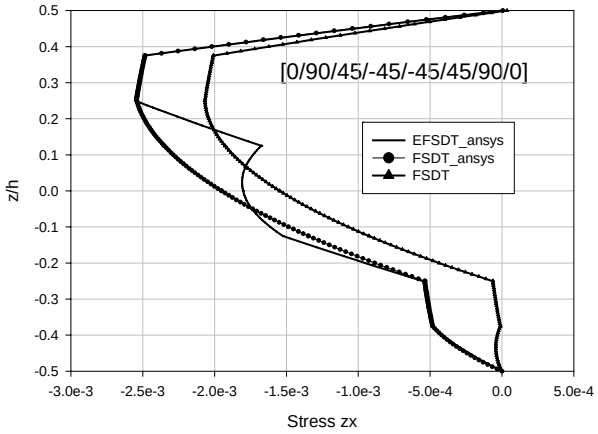

Fig. 5(a). Transverse shear stress zx under uniform loading

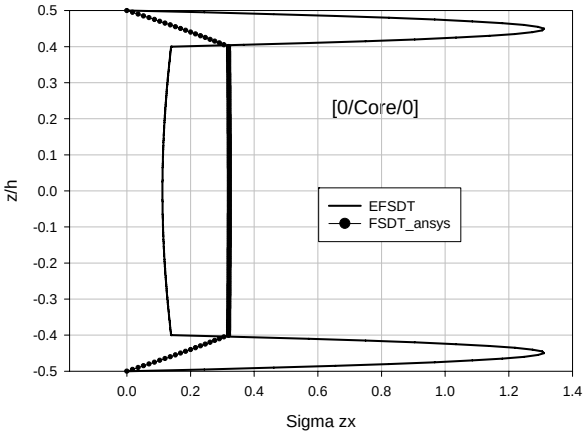

Fig. 6(b). Transverse shear stress zx $\bar{\sigma}_{zx} = \sigma_{zx} / q_0 S$ of sandwich plate under uniform loading

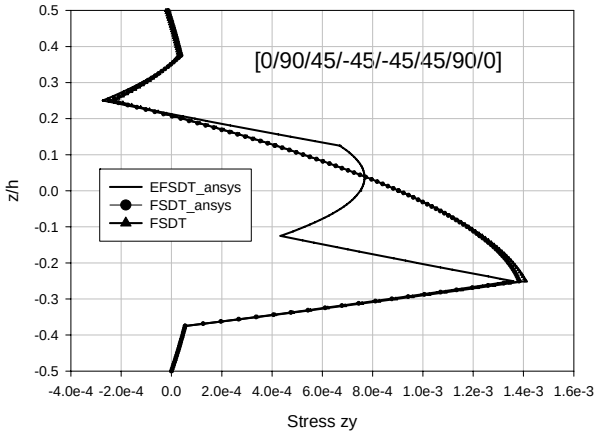

Fig. 5(b). Transverse shear stress zy under uniform loading

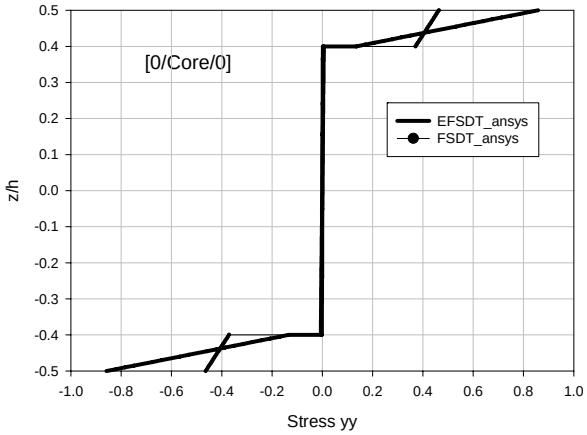

Fig. 6(a). In-plane stress yy $\bar{\sigma}_y = \sigma_y / q_0 S^2$ of sandwich plate under uniform loading